Journal of Power Sources 197 (2012) 154–160

Contents lists available at SciVerse ScienceDirect

Journal of Power Sources

journal homepage: www.elsevier.com/locate/jpowsour

Compliant alkali silicate sealing glass for solid oxide fuel cell applications: Combined stability in isothermal ageing and thermal cycling with YSZ coated ferritic stainless steels

Yeong-Shyung Chou*, E.C. Thomsen, J.-P. Choi, J.W. Stevenson

K2-44, Energy and Efficiency Division, Pacific Northwest National Laboratory, P.O. Box 999, Richland, WA 99354, United States

ARTICLE INFO

Article history:
Received 12 August 2011
Received in revised form 9 September 2011
Accepted 10 September 2011
Available online 16 September 2011

Keywords:
Sealing glass
Compliant glass
YSZ coating
SOFC

ABSTRACT

An alkali silicate glass (SCN-1) is being evaluated as a candidate sealant for solid oxide fuel cell (SOFC) applications. The glass contains about 17 wt.% alkalis (K + Na) and has low glass transition and softening temperatures. It remains vitreous and compliant after sealing without substantial crystallization, as contrary to conventional glass–ceramic sealant. The glassy nature and low characteristic temperatures can reduce residual stresses and result in the potential for crack healing. In a previous study, the glass was found to have good thermal cycle stability and was chemically compatible with yttria stabilized zirconia (YSZ) coating during short term testing. In this study, the compliant glass was further evaluated in a more realistic way in that the sealed couples were first isothermally aged for 1000 h followed by thermal cycling. High temperature leakage was measured. Chemical compatibility was also investigated with powder mixtures to enhance potential interfacial reaction. In addition, interfacial microstructure was examined with scanning electron microscopy and evaluated with regard to the leakage and chemical compatibility results. Overall the compliant sealing glass showed desirable chemical compatibility with YSZ coated metallic interconnect of minimum reaction and hermetic behavior at 700–750 °C in dual environment.

1. Introduction

Solid oxide fuel cells (SOFCs) are an emerging energy technology which has many advantages over existing technologies: high electrical conversion efficiency (over 60%), potential for carbon capture, no NOx emission, fuel flexibility, low noise, and flexibility for transportation and stationary applications [1–4]. To increase the volumetric power density, planar design SOFC, in which repeating flat unit cells are stacked and connected electrically in series, is the current leading candidate. Due to processing and quality control the size of ceramic cell is often limited to no more than 10–12 in. As a result, SOFC stacks must contain ~50 to ~100 of repeating cells to reach power output in the tens of kW range. This presents a great challenge in sealing since planar SOFCs require several different seals: ceramic cell to "window frame," interconnect plate to interconnect plate or window frame, and seals between end plates which provide gas inlets and outlets [5]. The very harsh SOFC operating conditions, i.e., elevated temperatures and dual environments, and requirement of a lifetime up to 40,000 h with hundreds to thousands of thermal cycles make seal development a most challenging hurdle [6].

To date, SOFC glass seal research has been focused mainly on glass–ceramic approaches in which the initial glass devitrifies into a rigid or semi-rigid glass–ceramic mixture after the sealing processes [7–22]. Most of the glass–ceramic approaches focused on alkaline earth-based silicate glasses, likely due to the fact that compositions can be modified to match coefficient of thermal expansion (CTE) with SOFC components [8–12,15,16]. Other systems, including phosphate glasses [14], borosilicate glasses [7], and ceramic fiber reinforced glass [8], have also been investigated. However, the CTEs of these non-alkaline earth based glasses were in the low range, e.g., ~5.7 to 7.9 × 10^{-6} °K^{-1} for the phosphate glasses, which resulted in poor thermal cycle stability [14].

Recently a novel approach involving compliant glass was proposed for SOFCs. The glass will remain vitreous without substantial crystallization after sealing and during operation at elevated temperatures. In contrast to the conventional glass–ceramic sealant which develops a rigid or semi-rigid microstructure after sealing, the compliant glass will retain the glassy nature and result in more tolerance in terms of residual stresses. Should cracking occur during routine thermal cycling, the capillary force or surface tension of the compliant glass at elevated temperatures would lead to a

* Corresponding author. Tel.: +1 509 3752527; fax: +1 509 3752186.
E-mail address: yeong-shyung.chou@pnl.gov (Y.-S. Chou).

0378-7753/$ – see front matter
doi:10.1016/j.jpowsour.2011.09.027

"self-healing" behavior [23–25]. Indeed, crack healing has been observed in glasses at elevated temperatures [25,26]. However, the ability to maintain a vitreous state without crystallization at SOFC operation conditions over the long term remains unknown. In our earlier work, we reported the initial investigation of a compliant alkali-containing silicate glass, with an emphasis on thermal property characterization and leak behavior during thermal cycling at various temperatures and back pressures [27]. The glass showed desirable thermal cycle stability over 20 deep thermal cycles at various temperatures from 700 to 800 °C, and minimum interfacial reaction was found along YSZ electrolyte and alumina coating interfaces. In the present work, the compliant glass was further studied in terms of combined isothermal ageing and deep thermal cycling to mimic the real SOFC stack operation conditions. Of particular interest is the chemical interaction with a potential coating candidate for ferritic stainless steels, i.e., YSZ. High temperature leak rate versus ageing time and deep thermal cycles will be reported. Interfacial microstructure characterization, evaluation of YSZ/glass powder mixtures for enhanced chemical reactions, and the possible reaction and the stability of YSZ protective coating will be discussed.

2. Experimental

2.1. Glass composition and thermal properties

The glass under study is a commercial alkali silicate glass (SCN-1, SEM-COM, Toledo, OH). It contains alkaline earths, mainly BaO (8.23 wt.%) and CaO (3.34 wt.%), alkalis of K_2O (10.0 wt.%) and Na_2O (7.3 wt.%), Al_2O_3 (2.8 wt.%), SiO_2 (66.9 wt.%) and some impurities (less than 1%) of Fe, Mg and Ti. The glass has a glass transition temperature of 468–486 °C, softening point of 540–600 °C, and average coefficient of linear thermal expansion (CTE) up to glass transition of $\sim 11 \times 10^{-6}\,°C\,K^{-1}$. The details of the thermal property characterization were given in Ref. [27].

2.2. Sample preparation and coupon sealing

To mimic actual SOFC conditions, the candidate sealing glass was sealed between a NiO/YSZ anode-supported thin YSZ electrolyte bi-layer and a ferritic stainless steel (SS441, ATI Allegheny Ludlum, Pittsburgh, PA) square substrate of 50 mm × 50 mm × 1 mm. The metal substrate was machined with a circular groove to contain the sealing glass. The details of ceramic bi-layer and metal substrate preparation are given in Ref. [27]. Stainless steel SS441 is currently considered a candidate metallic interconnect for planar SOFC applications, due to matching CTEs with NiO-YSZ anode, conductive oxide scale formation, and reasonable low cost. However, Cr from the metal can cause poisoning as well as mechanical degradation in sealing by forming chromates with very high CTEs [17,18,28]. As a result, a protective coating is required for the sealing area. In earlier work we have adopted a novel reactive air aluminizing coating process involving ultrasonic spraying of SS441 substrates with a mixture of Al powders in a binder solution, followed by drying and oxidizing at 1000 °C for 1 h in air [29]. However, due to potential reaction of alumina with sealing glass, a YSZ coating was applied in addition to the aluminization process. Fine YSZ powders were mixed with organic binders to form slurry and ultrasonically sprayed (Model Prism-350, USI, Haverhill, MA) a few times (in *x* and *y* directions) onto the aluminized substrate at room temperature. The substrate was then dried and heat treated at 1000 °C for 1 h in air. Fig. 1 shows the preparation of the test couples with glass paste on the SS441 substrate (Fig. 1A), and the joined couple after sealing at 800 °C for 2 h in air (Fig. 1B).

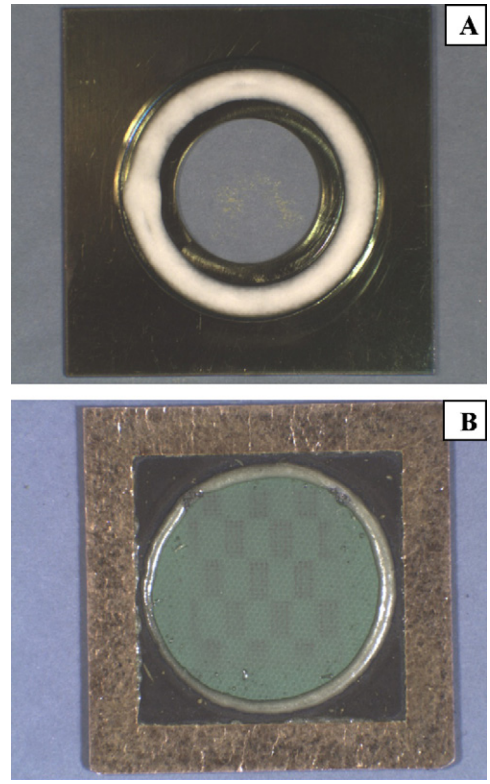

Fig. 1. Optical micrograph shows the sample preparation for coupon sealing. (A) White glass paste applied onto circular groove of SS441 substrate with a central hole for dual environment exposure, and (B) sealed green ceramic bilayers disc and metal substrate couple with mica perimeter seals (the use of mica perimeter seal is illustrated in Fig. 2).

2.3. Leak test, thermal cycling, ageing in dual environment, and characterization

The as-sealed couples (Fig. 1B) were first leak checked at room temperature using iso-propanol. Only hermetic samples, i.e., no alcohol penetration, were used for thermal cycle and isothermal ageing tests. The sample was then pressed at 82–163 kPa between a leak tester made of Inconel 600 and an alumina support as shown in Fig. 2. A hybrid mica seal with Ag or SCN-1 glass as the interlayer was used for the perimeter seal [6]. The sample was first isothermally aged for 1000 h at 700 or 750 °C followed by 5–10 deep thermal cycles from ∼50 °C to elevated temperatures with a heating rate of 5 °C min^{-1} and natural furnace cooling. A dilute fuel of 5% H_2 in N_2 (with ∼3% H_2O) was flowing inside the test chamber surrounded by ambient air. During isothermal ageing and thermal cycling, high temperature leak rates were measured with high-purity helium. The details of thermal cycling and leak test are given in Ref. [27]. After the test, the sample was checked with optical microscopy, followed by cutting and polishing for microstructure and chemical analysis with scanning electron microscopy (SEM) and energy dispersion spectroscopy (EDS) (JEOL SEM model 5900LV).

2.4. Chemical compatibility

To induce rapid chemical reaction between YSZ coating and the SCN-1 glass, powder mixtures were used. The as-received SCN-1 glass powder and YSZ powder (TOSOH ZIRCONIA, Japan, TZ-8YS, <1 μm) were mixed at a weight ratio of 1:1 in a 250 mL plastic jar with ZrO_2 milling cylinders and iso-propanol. The powder mixtures were ball milled for 1 h followed by drying on a hot-plate

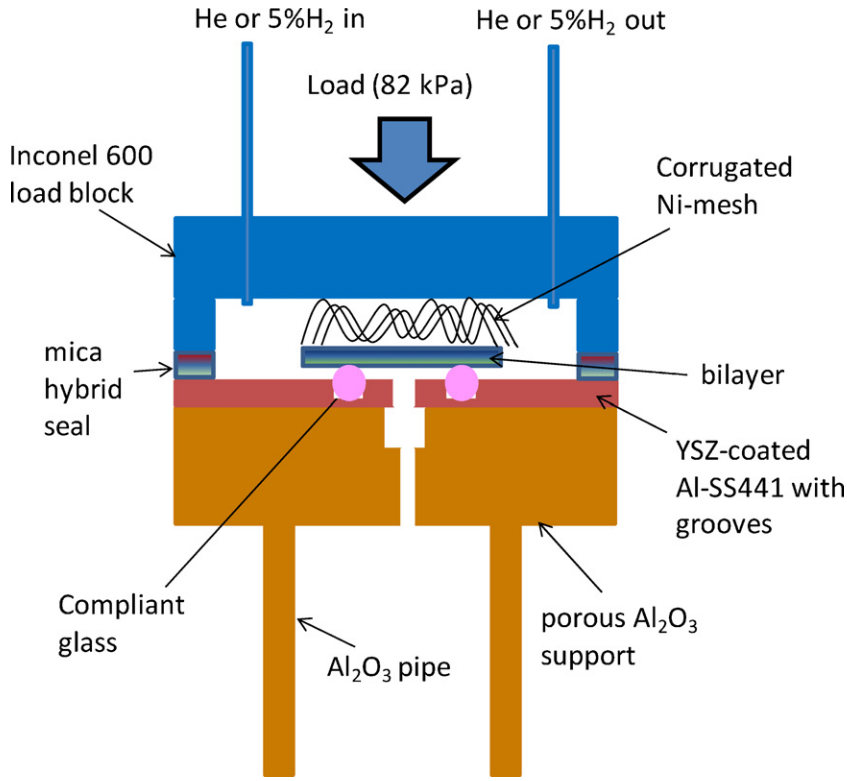

Fig. 2. Schematic drawing shows the assembly of leak test fixture for glass sealed between a ceramic bi-layer and an YSZ-coated aluminized SS441 substrate with grooves. The sample was pressed between an Inconel 600 top fixture and an alumina bottom support with hybrid mica as the perimeter seal. To mimic actual solid oxide fuel cells, a Ni-mesh was inserted on top of the cell.

with constant stirring to minimize the settling of large size SCN-1 glass powders. The mixed powders were then die-pressed into discs and fired to 800 °C for 2 h in air. The as-fired disks were further isothermally aged in ambient air at 700 and 800 °C for 1000 h as the lower and upper bound for this compliant glass. After ageing, the disks were crushed, ground, and sieved through #325 mesh for X-ray diffraction (XRD) characterization (Rigaku, Miniflex II, X-ray diffractometer, Japan).

3. Results and discussion

3.1. YSZ coating for SS441 metal substrate

In our earlier work evaluating thermal cycle stability with the compliant SCN-1 sealing glass, minimum interfacial reaction was observed with the dense YSZ electrolyte, as well as the alumina coating on the SS441 metal substrate [27]. However, a stable crystalline phase of $KAlSi_3O_8$, Sanidine monoclinic structure, did form when in mixed powders after isothermal ageing at 800 °C/1000 h [30]. The fact that the current silicate glass does contain an appreciable amount of K_2O makes it likely that interaction with an alumina coating will occur during the long-term operation. In addition, corrosion of alumina or alumina-containing refractory by alkalis to form β-alumina ($NaAl_9O_{14}$) has been investigated in sodium discharge lamp envelopes [31], composite and structure ceramics [32], and glass melting [33]. A YSZ coating was therefore investigated as an additional coating for the SS441 metal substrate. Selection of YSZ was motivated not only from the minimum reaction observed from previous work, but also by the considerations related to residual stresses and integrity of coating adhesion. Aluminization of stainless steel is a well established process, due to low melting point of metal Al which can be easy activated by halides, and fast diffusion into metal matrix. However, the very high elastic modulus (~400 GPa) and relatively low CTE (~8.8×10^{-6} °K^{-1}) can lead to large residual stresses when coated onto a SS441 substrate which has a high CTE of ~12.5×10^{-6} °K^{-1}. The combination of these two materials can result in de-lamination if coating thickness is not optimized. From a residual stress point of view, YSZ coating should be favored over Al_2O_3 coating since YSZ has a lower elastic modulus (~200 GPa) and higher CTE (~10.5×10^{-6} °K^{-1}). As a result, the residual stresses should be significantly lower than alumina coating. However, direct coating of YSZ onto bare SS441 substrates resulted in poor adhesion; the coatings either did not adhere or spalled off after a few thermal cycles. Whether the cause was due to limited chemical bonding/diffusion of Zr with SS441 or lack of mechanical interlocking (since the substrate surface was rather smooth) remains to be investigated. Therefore, YSZ coatings were applied to pre-aluminized SS441. Fig. 3 shows the typical microstructure of the YSZ coating on the aluminized SS441

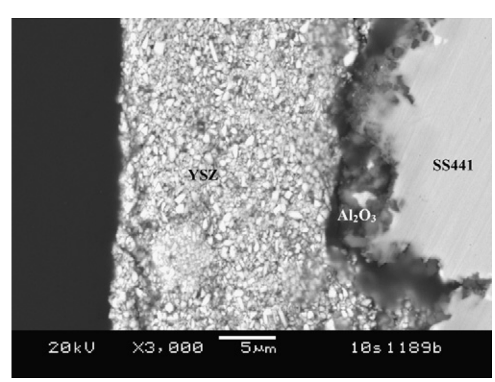

Fig. 3. Typical microstructure of YSZ-coated aluminized SS441 substrate showing the relatively porous thick YSZ coating and thin Al_2O_3 layer.

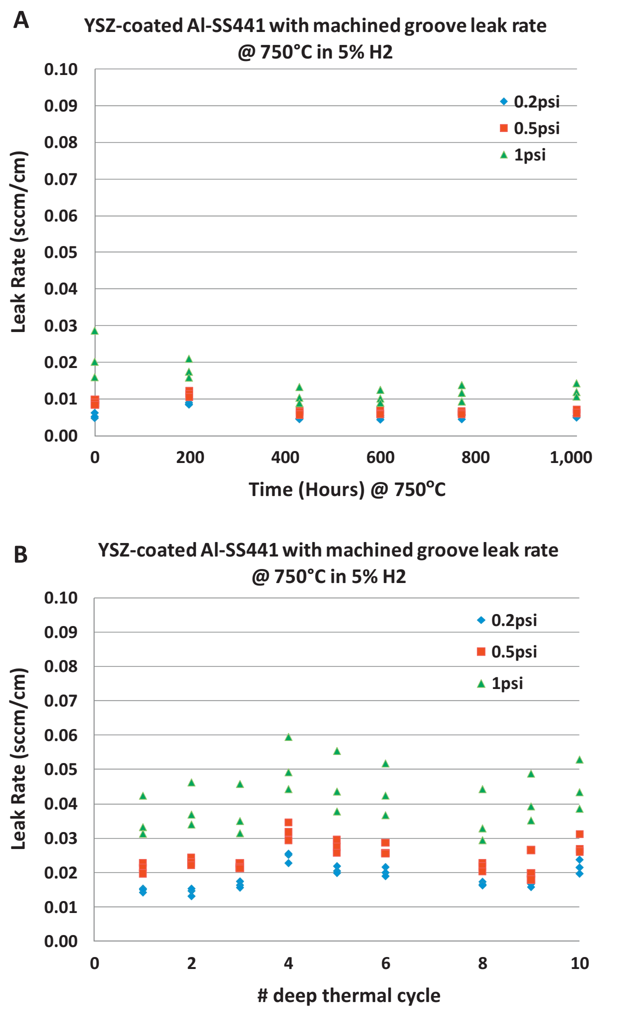

Fig. 4. High temperature leakage of SCN-1 glass with YSZ coated aluminized SS441 substrate. (A) Isothermal ageing at 750 °C, and (B) 10 deep thermal cycles (after isothermal ageing).

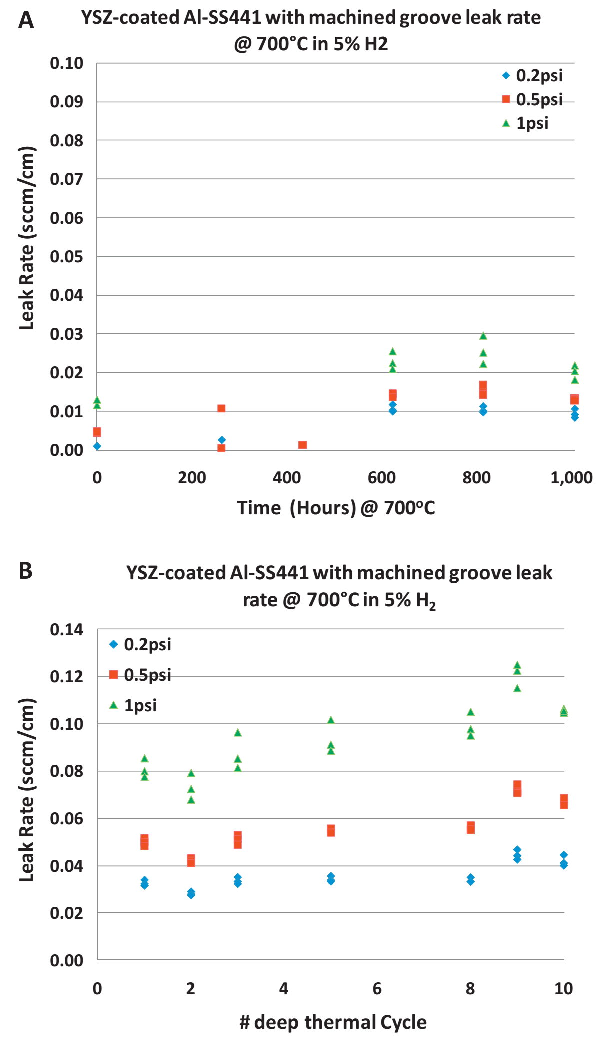

Fig. 5. High temperature leakage of SCN-1 glass with YSZ coated aluminized SS441 substrate. (A) Isothermal ageing at 700 °C, and (B) 10 deep thermal cycles (after isothermal ageing).

substrate. The YSZ coating was rather porous and thick, with thickness around 25–30 μm, due to multiple spray runs (6 times) to ensure full coverage of the alumina layer. The alumina coating was thin (a few microns thick) and appeared to be continuous. The original smooth metallic surface was roughened during the aluminization process at 1000 °C for 1 h.

3.2. Combined isothermal ageing and thermal cycling

As mentioned earlier, SOFC stacks are expected to operate at elevated temperature for long periods of time (up to 40,000 h) with many thermal cycles during routine operation. The current glass has a low viscosity of 10^5 Pa s at 800 °C, $10^{5.5}$ Pa s at 750 °C, and $10^{6.5}$ Pa s at 700 °C. At 700 °C the viscosity is equivalent to the softening point of common glass by its own weight [34]. The interaction of sealing glass, especially the soft or paste-like compliant glass with appreciable amount of alkalis, with mating materials is of particular interest. Any undesirable interfacial reaction can potentially lead to the degradation of seal integrity. Our earlier work reported the effect of thermal cycling tests in which the accumulated time at elevated temperature was rather short (~60 h for a total of 20 thermal cycles). The current work, which combined isothermal and thermal cycle testing, was intended to shed more light on the viability of the compliant sealing glass. Fig. 4 shows the high temperature leak rates during the combined stability test, which consisted of a first stage of isothermal ageing at 750 °C for 1000 h (Fig. 4A) followed by a series of deep thermal cycles (Fig. 4B). Fig. 5 shows the similar results for samples tested at 700 °C. It is evident that the leak rates appeared to be constant during the initial 1000 h ageing for both 700 and 750 °C tests, with leak rates in the range of 0.01–0.02 standard cubic centimeter per minute per cm leak length (sccm cm^{-1}, at 1.4 kPa). This is the typical leak rate for the hybrid mica seals (used as perimeter seals in the test fixture) under a compressive stress of 82 kPa [6,27], clearly suggesting the hermetic nature of the seal over the 1000 h ageing. During the following 10 thermal cycles, the leak rate slightly increased, with slightly higher leak rates observed for 700 °C samples than 750 °C ones. Nonetheless, the leakages were still within the nominal leak rates for hybrid micas (0.01–0.04 sccm cm^{-1} at 1.4 kPa differential gas pressure) and remained fairly constant, demonstrating the desired stability and hermetic nature. Although the interpretation of hermeticity from leak rates was indirect, the samples were all tested with iso-propanol at the end of test and no penetration was found.

3.3. Interfacial microstructure characterization

After the combined test, samples were mounted, cut and polished for microstructure characterization. Fig. 6 shows the typical

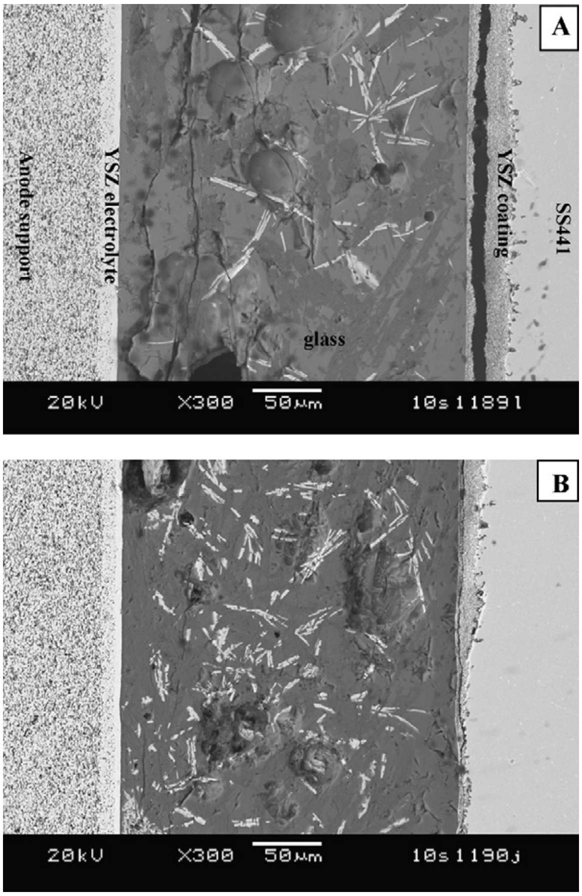

Fig. 6. Microstructure of SCN-1 glass sealed between anode-supported YSZ bilayer and YSZ-coated aluminized SS441 substrate after (A) isothermal ageing at750 °C for 1000 h and (B) 700 °C for 1000 h followed by 10 deep thermal cycles.

microstructure across the two YSZ interfaces of the sample after annealing at 750 °C for 1000 h (Fig. 6A) and 700 °C for 1000 h (Fig. 6B) and 10 deep thermal cycles. The glass appears bonded with both the dense YSZ electrolyte and the porous YSZ coating. There was fracture through the thick YSZ coating (Fig. 6A). This likely occurred during metallurgical sample preparation, not during the combined stability test, otherwise high leak rates would be anticipated. The weakness of the YSZ coating is not surprising since multiple coating runs were applied to build up the thick layer, and between each runs the coated powder slurry needed to be dried. In addition, the heat-treatment for the YSZ coating was carried out at the relatively low temperature of 1000 °C. At such a low temperature, solid-state sintering between YSZ particles would be minimal. It is also interesting to note that the fracture did not propagate along the YSZ/alumina interface where the solid-state sintering/bonding would be expected to be similarly weak, due to CTE mismatch and the fact that the nominal sintering temperature of Al_2O_3 and YSZ are very similar. This is likely due to the mechanical interlocking at the rough Al_2O_3 surface.

Looking at the glass microstructure, it is clear that the glass did partially crystallize, as evidenced by some white rod-like precipitates, and some light gray precipitates. There were more white precipitates for 700 °C sample than 750 °C one. At high magnification along the YSZ electrolyte interface of the 750 °C sample (Fig. 7), it is evident that the glass was chemically compatible with YSZ electrolyte in that no distinct precipitates or crystallites could be identified. Also the YSZ/glass interface was rather smooth, indicating no substantial corrosion by the glass or YSZ grains dissolution into the glass matrix. Energy dispersive spectroscopy was

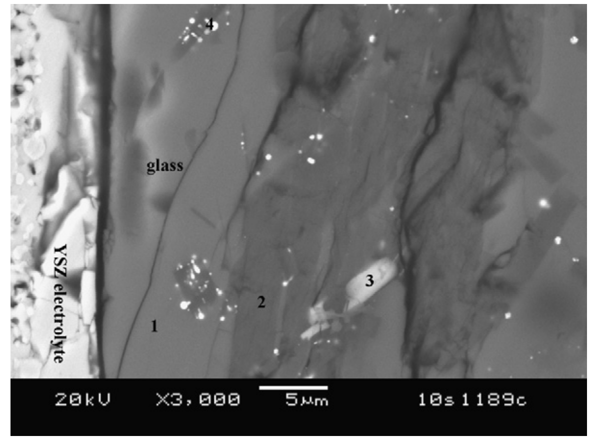

Fig. 7. High magnification of microstructure along YSZ (electrolyte) and SCN-1 glass interface after isothermal ageing at 700 °C for 1000 h and 10 deep thermal cycles. Note minimum interaction of the glass with YSZ.

conducted on selected spots and the chemical analysis in atomic% is listed in Table 1. Inside the glass matrix close to the YSZ electrolyte (spot 1 in Fig. 7), EDS showed a trace amount of Zr, likely from the parent glass. The light gray precipitates (spot 2 in Fig. 7) contained an appreciable amount of the alkalis, Ca and Si. However, the atomic ratio does not correspond to $KAlSi_3O_8$ phase. The white particles (spot 3 in Fig. 7), which contained primarily Ba and Si with small amounts of Na and K, could be $BaSiO_3$. Some very tiny white particles were also identified (spot 4 in Fig. 7) which contained some Ag and Sb, likely from the Ag/mica hybrid mica used for perimeter seals. To further investigate the interaction or diffusion across the interface, line scans were conducted across the YSZ electrolyte/glass and YSZ coating/glass interface as shown in Figs. 8 and 9, respectively. Clearly the inter-diffusion of YSZ and glass constituents was very limited, indicating the desired stability. Some precipitates were also observed along the YSZ coating/glass interface (Fig. 9) but these precipitates showed similar contrast and morphology to those inside the glass matrix.

3.4. Chemical compatibility with powder mixture

In addition to the combined stability test with YSZ electrolyte and YSZ coating, the chemical compatibility was further investigated using direct powder mixtures in which fine (<1 μm) YSZ powders were used. The goal was to accelerate the reaction, if any, since the YSZ electrolyte was previously sintered at a much higher temperature ∼1450 °C such that the chemical potential for sintering (as well as for reaction) was likely reduced. On the other hand, the YSZ coating was heat treated at 1000 °C but have a slightly larger particle size and small contact area for substantial reaction. The

Table 1
Chemical analysis of selected spots in Fig. 7 in at.% of sample after annealing at 750 °C for 1000 h with 10 thermal cycles in dual environment.

Element\spot	1	2	3	4
O K	57.9	58.85	55.83	57.85
Na K	5.62	5.37	2.23	2.86
Mg K	0.66	0.27	ND	0.51
Al K	1.28	0.20	0.96	4.21
Si K	26.71	25.13	29.91	23.62
K K	4.43	5.16	2.17	4.71
Ni K	ND	ND	ND	0.32
Ag L	ND	ND	ND	2.84
Sb L	ND	ND	ND	2.41
Ca K	1.12	4.85	1.10	ND
Zr L	0.66	ND	ND	ND
Ba L	1.62	0.17	7.79	0.67

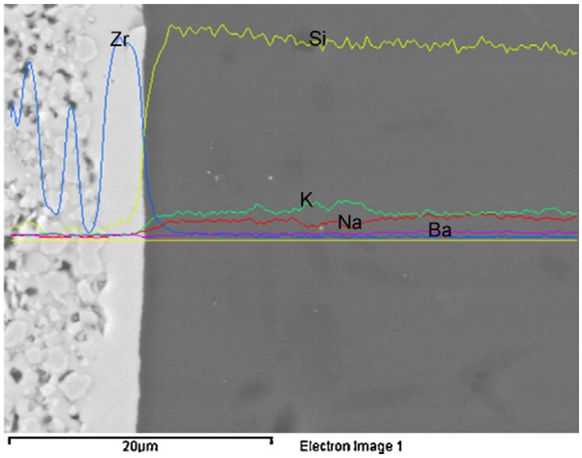

Fig. 8. Line scan across YSZ electrolyte and SCN-1 glass interface after isothermal ageing at 750 °C for 1000 h followed by 10 deep thermal cycles in dual environment.

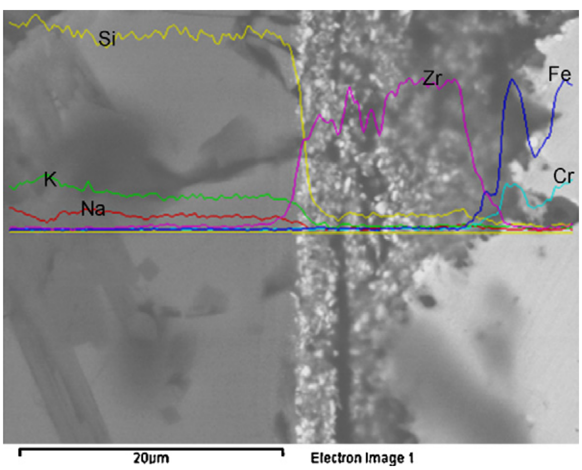

Fig. 9. Line scan across YSZ coating and SCN-1 glass interface after isothermal ageing at 750 °C for 1000 h followed by 10 deep thermal cycles in dual environment.

X-ray diffraction pattern for the mixed powder approach is shown in Fig. 10 for the 800 °C annealed for 1000 h and 700 °C for 1000 h samples, as well as the glass after initial sealing process (800 °C for 2 h). It is evident the SCN-1 glass was amorphous without any distinct crystalline peaks. The sample aged at 700 °C showed only the cubic YSZ peaks. Similar results were obtained for the 800 °C sample; however, there were a few un-identified crystalline peaks of small amount. The current XRD results are consistent with previous SEM and EDS analysis indicating that the YSZ coating and electrolyte are chemically compatible with the alkali-containing SCN-1 glass.

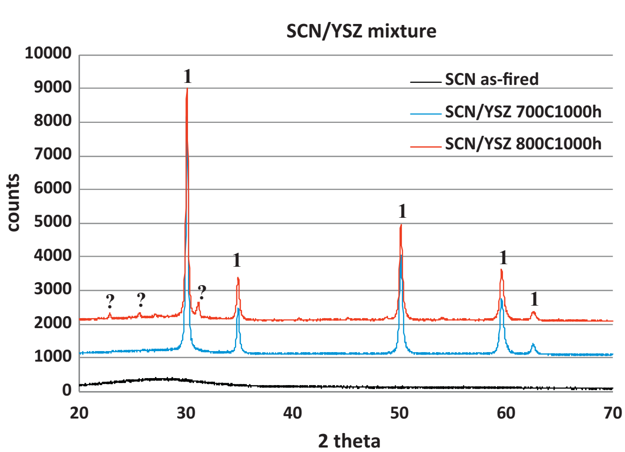

Fig. 10. XRD patterns of glass/YSZ powder mixture (weight ratio of 1:1) after isothermal ageing at 700 and 800 °C for 1000 h in air. For comparison the diffraction pattern of sintered glass (800 °C for 2 h) is also included (1 = cubic YSZ).

4. Summary and conclusions

A novel alkali-containing compliant silicate sealing glass for SOFC applications was evaluated in terms of combined isothermal ageing and deep thermal cycling at 700 and 750 °C in dual environment. The compliant glass was sealed between anode-supported YSZ electrolyte and YSZ coated aluminized SS441 metal substrate. The high temperature leak tests showed that all samples exhibited good combined stability (isothermal ageing and 10 deep thermal cycles) with hermetic seal behavior. From interfacial microstructure analyses and XRD of powder mixtures, the alkali-containing glass was found to be chemically compatible with YSZ electrolyte as well as the YSZ coating in that no discernable reaction or dissolution was found. The thick YSZ coating, however, presents a potential for fracture and further optimization is required. Overall the current study demonstrated the applicability of a compliant sealing glass for SOFC sealing applications with YSZ ceramics.

Acknowledgements

The authors would like to thank S. Carlson and J. Coleman for SEM sample preparation and analysis. This paper was funded through the US Department of Energy's Solid-State Energy Conversion Alliance (SECA) Core Technology Program. Pacific Northwest National Laboratory is operated by Battelle Memorial Institute for the US Department of Energy under Contract no. DE-AC06-76RLO 1830.

References

[1] N.Q. Minh, J. Am. Ceram. Soc. 76 (3) (1993) 563–588.
[2] S.S. Tam, 11th Annual SECA Workshop, Pittsburgh, PA, July 27–29, 2010.
[3] B.C.H. Steele, A. Heinzel, Nature 414 (6861) (2001) 345–352.
[4] M.C. Williams, J.P. Strakey, W.A. Surdoval, J. Power Sources 143 (1–2) (2005) 191–196.
[5] Y.-S. Chou, J.W. Stevenson, J.-P. Choi, Int. J. Appl. Ceram. Technol. 123 (2) (2010) 1–10.
[6] Y.-S. Chou, J.W. Stevenson, J. Mater. Eng. Perform. 15 (4) (2006) 414–421.
[7] X. Qi, F.T. Akin, Y.S. Lin, J. Membr. Sci. 193 (2) (2001) 185–193.
[8] S. Taniguchi, M. Kadowaki, T. Yasuo, Y. Akiyama, Y. Miyake, K. Nishio, J. Power Sources 90 (1) (2000) 163–169.
[9] K.L. Ley, M. Krumpelt, R. Kumar, J.H. Meiser, I. Bloom, J. Mater. Res. 11 (6) (1996) 1489–1493.
[10] V.A.C. Haanappel, V. Shemet, I.C. Vinke, S.M. Gross, T.H. Koppitz, N.H. Menzler, M. Zahid, W.J. Quadakkers, J. Mater. Sci. 40 (7) (2005) 1583–1592.
[11] N. Lahl, D. Bahadur, K. Singh, L. Singheiser, K. Hilpert, J. Electrochem. Soc. 149 (5) (2002) A607–A614.
[12] N. Lahl, K. Singh, L. Singheiser, K. Hilpert, D. Bahadur, J. Mater. Sci. 35 (12) (2000) 3089–3096.
[13] S.-B. Sohn, S.-Y. Choi, G.-H. Kim, H.-S. Song, G.-D. Kim, J. Non-Cryst. Solids 297 (2–3) (2002) 103–112.
[14] P.H. Larsen, P.F. James, J. Mater. Sci. 33 (10) (1998) 2499–2507.
[15] K.D. Meinhardt, D.-S. Kim, Y.-S. Chou, K.S. Weil, J. Power Sources 182 (1) (2008) 188–196.
[16] S.-E. Lin, Y.-R. Cheng, W.C.J. Wei, J. Eur. Ceram. Soc. 31 (11) (2011) 1975–1985.
[17] Y.-S. Chou, J.W. Stevenson, P. Singh, J. Electrochem. Soc. 154 (7) (2007) B644–B651.
[18] Y.-S. Chou, J.W. Stevenson, K.D. Meinhardt, J. Am. Ceram. Soc. 93 (3) (2010) 618–623.
[19] Y.-S. Chou, J.W. Stevenson, G.-G. Xia, Z.-G. Yang, J. Power Sources 195 (17) (2010) 5666–5673.
[20] Y.-S. Chou, J.W. Stevenson, J.-P. Choi, J. Electrochem. Soc. 157 (3) (2010) B348–B353.
[21] P.K. Ojha, S.K. Rath, T.K. Chongdar, N.M. Gokhale, A.R. Kulkarni, J. Power Sources 196 (11) (2011) 4594–4598.
[22] M.K. Mahapartra, K. Lu, J. Power Sources 196 (2) (2011) 700–708.
[23] R.N. Singh, Int. J. Appl. Ceram. Technol. 4 (2) (2007) 134–144.

[24] J. Massera, J. Remond, J. Musgraves, M.J. Davis, S. Misture, L. Petit, K. Richardson, J. Non-Cryst. Solids 356 (52–54) (2010) 2947–2955.
[25] W.N. Liu, X. Sun, M.A. Khaleel, J. Power Sources 196 (4) (2011) 1750–1761.
[26] B.A. Wilson, E.D. Case, J. Mater. Sci. 32 (3) (1997) 3163–3175.
[27] Y.-S. Chou, E.C. Thomsen, R.T. Williams, J.-P. Choi, N.I. Canfield, J.E. Bonnett, J.W. Stevenson, A. Shyam, E. Lara-Curzio, J. Power Sources 196 (5) (2011) 2709–2716.
[28] Z. Yang, J.W. Stevenson, K.D. Meinhardt, Solid State Ionics 160 (1) (2003) 213–225.
[29] J.-P. Choi, K. Scott Weil, Y.-S. Chou, J.W. Stevenson, Z.-G. Yang, Int. J. Hydrogen Energy 36 (7) (2011) 4549–4556.
[30] Y.-S. Chou, unpublished work.
[31] J.A.M. van Hoek, F.J.J. van Loo, R. Metselaar, J. Am. Ceram. Soc. 75 (1) (1992) 109–111.
[32] S.K. Sundaram, J.-Y. Hsu, R.F. Speyer, J. Am. Ceram. Soc. 77 (6) (1994) 1613–1623.
[33] K.E. Spear, M.D. Allendorf, J. Electrochem. Soc. 149 (12) (2002) B551–B559.
[34] W. Vogel, Chemistry of Glass, American Ceramic Society Inc., OH, 1985, p. 23.